Contents lists available at ScienceDirect

### **Extreme Mechanics Letters**

journal homepage: www.elsevier.com/locate/eml



## A machine learning-based method to design modular metamaterials



Lingling Wu <sup>a,b,1</sup>, Lei Liu <sup>b,1</sup>, Yong Wang <sup>c</sup>, Zirui Zhai <sup>b</sup>, Houlong Zhuang <sup>b</sup>, Deepakshyam Krishnaraju <sup>b</sup>, Qianxuan Wang <sup>a</sup>, Hanqing Jiang <sup>b,\*</sup>

- <sup>a</sup> College of Railway Engineering, Wuyi University, Jiangmen, 529020, China
- <sup>b</sup> School for Engineering of Matter, Transport and Energy, Arizona State University, Tempe, AZ 85287, USA
- <sup>c</sup> Department of Engineering Mechanics, Zhejiang University, Hangzhou, Zhejiang, 310027, China

#### ARTICLE INFO

Article history:
Received 30 January 2020
Received in revised form 26 February 2020
Accepted 29 February 2020
Available online 7 March 2020

Keywords: Modular metamaterials Structural evolution Mechanical metamaterials Machine learning

#### ABSTRACT

The concept of modular metamaterials and a machine learning-based method are introduced in this Letter. The method starts from selection of the structural bases based on the existing studies and then combines performance evaluation together with structural evolution to construct meta-atoms with specified properties. Both genetic algorithm and neural networks model are adopted to executed the designing process. Mechanical metamaterials with maximized bandgap and tunable bandgaps are demonstrated using the proposed method. This approach offers an effective means to design metamaterials. It is believed that the modular design of metamaterials based on machine learning is capable to construct meta-atoms with specific properties for metamaterials in various fields.

© 2020 Elsevier Ltd. All rights reserved.

### 1. Introduction

Metamaterials exhibit extraordinary macroscopic properties resulted from the collective response of the periodically constructed meta-atoms rather than the individual ones [1-5]. By analogy with the representative volume elements in continuum mechanics [6], on the one hand meta-atoms possess elaborated structures, and on the other hand act as a fundamental element thoroughly governing the macroscopic performances of metamaterials. Thus, in the field of metamaterials, creation of various meta-atoms with specific internal structures possesses a pivotal role in the discovery of metamaterials with designated characteristics. The exceptional properties of metamaterials that have been realized include negative index [1,3,7,8], cloaking [4,9,10], perfect lens [11], negative Poisson's ratio [12-15], negative thermal expansion [16–19], to state only a few [5,20,21]. Specifically, in the field of phononic metamaterials [22-27], the main objective lies in constructing phononic meta-atoms to manipulate the propagation of elastic/acoustic waves. Remarkable performances have been achieved, including acoustic cloaking [28,29], negative refraction [30,31], sub-wavelength imaging [32,33], acoustic nonreciprocity [34], among many others.

There are two mainstream design methods to create metaatoms, i.e., the *ad hoc* method and the topology optimization [35–39]. The *ad hoc* method depends on gradually accumulated experiences and always requires a eureka moment, which may not lead to inheritable methodology. Topology optimization is a well-established mathematical method to spatially optimize the material layout within a given design space, and has achieved great success in designing metamaterials. Though topology optimization is easy to operate, a certain degree of blindness of its starting point makes this method computational expensive. Additionally, fabrication is sometimes difficult when complex models are obtained by topology optimization. In the field of phononic metamaterial, the ad hoc designs have achieved mass-in-mass structures [40], membrane-type structures [41-43], Helmholtz cavity resonators [2,44], and so on. On one hand, achievements obtained by the ad hoc design, though great, remain fragmented given that the ad hoc design does not provide a general methodology. On the other hand, the ad hoc method has led to accumulated knowledge based on the case-by-case studies to design metamaterials with diverse performance, similar to the development of period table of elements after centuries of exploration of discrete elements.

Inspired by the concept of *materials genome* [45,46], here we propose the concept of *modular metamaterials*. The core of the present method is the basis unit, or the modular unit. In biology, the terminology "genetics" associates with its basis unit, namely genes, which are a length of DNA. Each gene consists a string of many *modular* chemical building molecules, namely nucleotides, of which there are only four biological bases (i.e., adenine "A", thymine "T", guanine "G", and cytosine "C", in Fig. 1a). Rich biodiversity is rooted to various combinations of these bases. This modular design has inspired applications in other areas, including Lego toys, modular robots [47], and heterogeneously architected

<sup>\*</sup> Corresponding author.

E-mail addresses: ypwang@zju.edu.cn (Y. Wang), zzhai4@asu.edu (Z. Zhai), hanqing.jiang@asu.edu (H. Jiang).

<sup>&</sup>lt;sup>1</sup> Equal contribution.

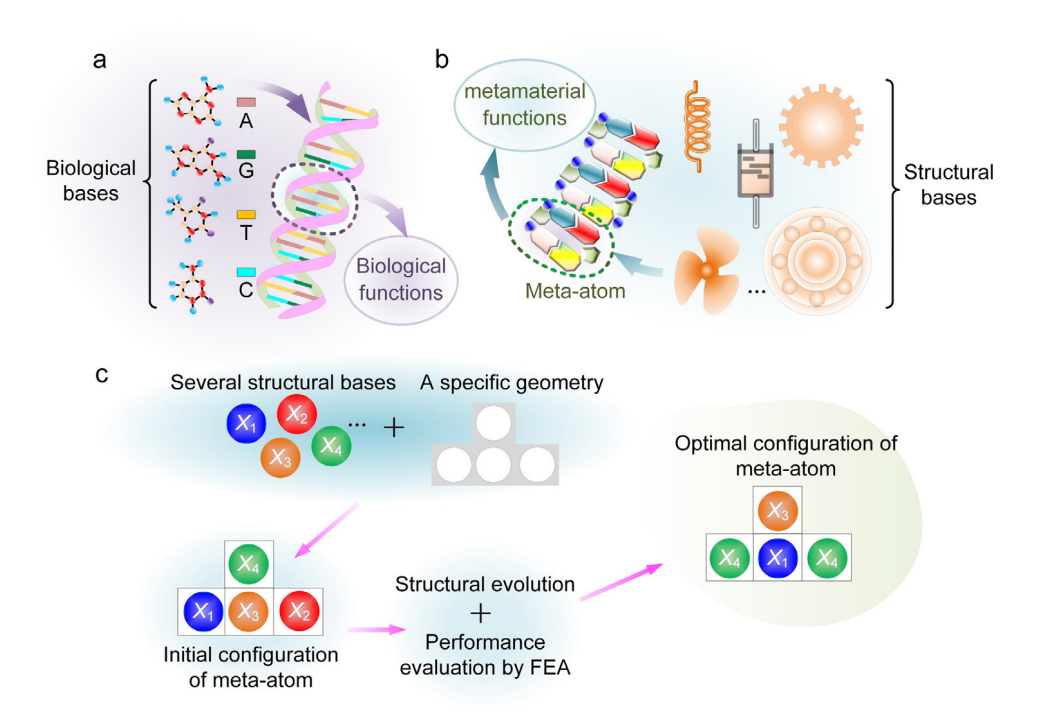


Fig. 1. Schematic of (a) biological genome and (b) modular design of meta-atoms; (c) Schematic of machine learning-based method to design modular metamaterials.

2D structures [48]. Thanks to the existing studies in the area of metamaterials using either the ad hoc design or topology optimization, useful bases have been discovered. In this Letter, we introduce a machine learning-based method to create modular metamaterials with specified performances, as shown in Fig. 1b. This successfully takes the advantages of the existing knowledge in metamaterials and provides a novel route to create metaatoms with desired performance. It starts from structural bases that are appropriately selected based on existing knowledge, and thus could save calculation time and is less time-consuming, which balances the design performances and computational cost, i.e., rapidly design metamaterials with sub-optimal performances with a small cost. The fabrication problem is also solved from the beginning when structural bases are selected. The following examples are studied to show the implementation of the modular design method: one-dimensional (1D) and two-dimensional (2D) mechanical metamaterials with maximized bandgap, maximized range of tunable bandgaps, and interconnection meta-atom for stretchable electronics with specific figure of merit.

#### 2. General methodology of modular metamaterial design

For a specified performance, the general methodology of metamaterial modular design includes two steps, i.e., step 1: the selection of basic components, and step 2: the iteration of performance evaluation and structural evolution, as shown in Fig. 1c. Step 1: number of basic components (hereinafter called "structural bases") are selected based on the existing studies. The chosen structural bases have related properties to the required performance of the to-be-designed meta-atom. Specific geometry is also prescribed, for example, 1D or 2D, to place the structural bases in a certain arrangement. Different arrangements define different meta-atoms. Step 2: Through sequential iteration between performance evaluation of the meta-atoms with a given arrangement using available methods (e.g., finite element analysis) and the structural evolution using various means (e.g., genetic algorithm or machine learning), a meta-atom with an optimal arrangement of structural bases for the required performance is thus achieved. Due to the attribute of modular property and the preselection of structural bases based on the existing knowledge, the modular design methodology is a computational-effective to design metamaterials. This approach could combine the advantages of topology optimization and *ad hoc* designs: *ad hoc* designs could provide a library of existing structural bases while topology optimization helps to search for the optimal arrangement of the preselected structural bases.

# 3. Examples: modular design of four meta-atoms with various performance

In this section, four examples are given to show the implementation of the present method to design meta-atoms: designing phononic meta-atoms with the objectives to achieve broader or tunable bandgaps [49], as well as the optimization of interconnects for stretchable electronics with a specific figure of merit.

The structural bases were chosen based on the knowledge from the existing studies. Finite element analysis was carried out for the performance evaluation of the meta-atom candidates. The structural evolution process was performed to find out the optimal meta-atom. Here, we used the genetic algorithm (GA) and neural networks (NN) model as the machine learning methods. GA could be readily combined with the COMSOL Multiphysics finite element simulations via LiveLink<sup>TM</sup> for MATLAB®. The schematic of the GA process is shown in Fig. S1, and details could be find in the literature [50]. By applying GA, a population size of meta-atoms is initially generated with each representing a candidate to the problem. Then, the genetic algorithm is employed to find out an optimal solution by genetically breeding a population of individuals over a series of generations until the change of fitness function between two adjacent generations is smaller than the tolerance [50]. Machine learning was also employed in these examples, which could be processed by the neural networks model with details in the supporting information. It must be pointed out that the structural evolution can be conducted in other means, not limited to GA or NN, but by

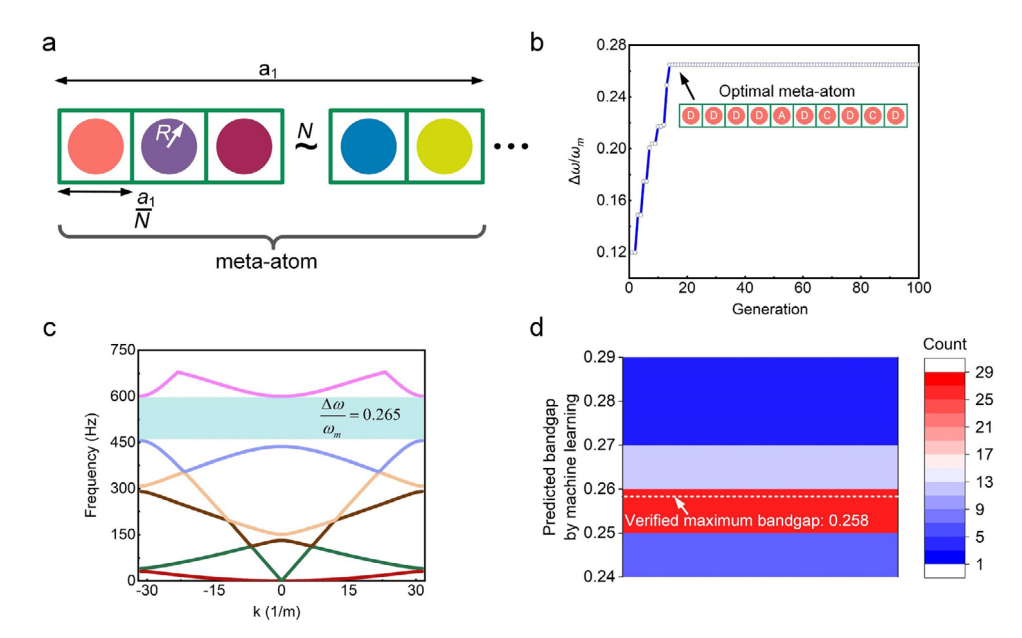


**Fig. 2.** Meta-atom with maximized relative bandgap based on four structural bases with circular inclusions embedded in a square matrix. (a) A meta-atom consisting of *N* structural bases with circular inclusions inside a square matrix. (b) The evolution of the relative bandgap using the genetic algorithm (GA). The inset shows the configuration of the optimal meta-atom. (c) Bandgap structure of the optimal meta-atom obtained by GA optimization. (d) The predicted result produced by machine learning. The contour shows the number of configurations predicted by the machine learning method. The dashed line indicates the maximum bandgap as verified by the finite element simulation.

other methods as well, such as colony optimization, simulated annealing and so on.

Four case studies are the following. (Case I) Designing a 1D metamaterial with maximized relative bandgap among the first six bands. (Case II) Designing a 1D metamaterial with maximized tunable bandgap region among the first six bands under 50% strain. (Case III) Designing a 2D metamaterial with maximized relative bandgap among the first six bands. (Case IV) Designing an optimal interconnect for stretchable electronics with a specific figure of merit. It should be noted that, these examples are selected solely to demonstrate the implementation of the present approach and their practical importance is not concerned. One can readily change the geometry and/or fitness function for their designated properties.

# 3.1. Case I: Maximizing relative bandgap for 1D phononic metamaterials

For Case I (Fig. 2a), a meta-atom consisting of N unit cells was constructed and each unit cell (i.e., the structural base) is a square matrix embedded with a circular inclusion as suggested by the existing studies [51–53], in which these structures have presented phononic bandgap properties. The material for the matrix is fixed, while that for the inclusions is to be determined. Four candidate materials (A, B, C, and D) for the inclusion was provided, and their properties are listed in Fig. S2a. Although only four candidate materials are provided, a great quantity ( $4^N$ ) of meta-atom configurations could be constructed. In this study case, N was set to be 10. The periodicity  $a_1$  of the simulated models equates 80 mm and the radius of the circular inclusion R is 3.5 mm. The population size of 30 was used, which means there are 30 finite element simulations in each generation to evaluate the band structure

The relative width of bandgap was selected as the fitness function for the optimization process, which is defined as the ratio between the bandgap width and its corresponding midgap frequency. The bandgap for a specific structure is calculated by the difference between the maximized value of the *j*th band

and minimum value of the j+1th band. Therefore, the fitness function  $f_1$  was given by

$$f_1 = \max \left\{ \frac{\min(\omega_{j+1}) - \max(\omega_j)}{\frac{\min(\omega_{j+1}) + \max(\omega_j)}{2}} \right\} \qquad j = 1, 2, 3 \dots$$
 (1)

where  $\omega_j$  and  $\omega_{j+1}$  are the frequencies of jth and j+1th bands, respectively. For the sake of simplicity, we only considered the first six bands in this example.

The GA calculation process is shown in Fig. 2b, from which one can see that a maximized fitness function value of 0.265 was obtained in the 14th generation. Given that there are 30 populations in each generation, one only needs  $30 \times 14 = 420$  finite element simulations to achieve the maximized configuration, which is only a very small fraction (i.e., 0.04%) of the total possible configurations ( $4^{10} = 1,048,576$ ), which shows the efficiency of this modular design method. The structure of the optimal meta-atom with relative bandgap of 0.265 is shown in the inset of Fig. 2b. Based on this meta-atom, a 1D phononic metamaterial with maximized relative bandgap could be constructed. Its band structure with a wide bandgap between [458 Hz, 598 Hz] is shown in Fig. 2c. In order to show that the present modular design method can use other evolution algorithm, we also carried out the optimization process by adopting the neural network method. Here, we randomly generated 1000 configurations of the meta-atoms and calculated the relative width of the bandgap (e.g., Eq. (1)). Using these 1000 data as the samples for training and testing, the neural network method predicts combinations that might have optimal performance. Detailed calculation process is provided in the supporting information. From the prediction result shown in Fig. 2d, we can see that a maximized relative bandgap of 0.258 was predicted, which closely agrees with the result obtained from the GA process.

# 3.2. Case II: Maximizing tunable bandgap region under 50% strain for 1D phononic metamaterials

In this example, the structural bases was composed of a square matrix with different voids, which have shown to possess tunable

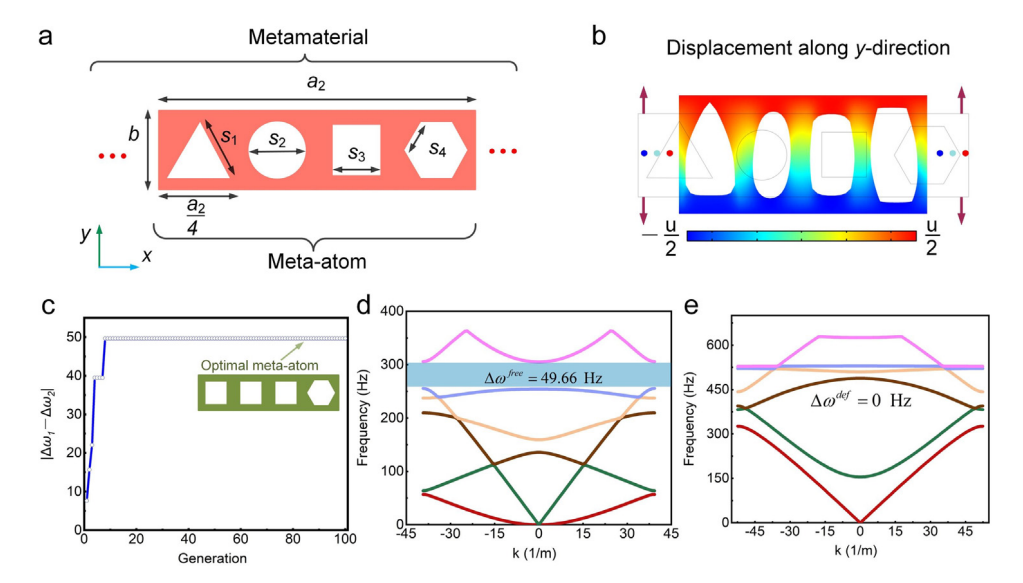


**Fig. 3.** A tunable phononic bandgap by applying a uniaxial tension strain. (a) Schematic of an arbitrary mechanical metamaterial model at free state. (b) Configuration of the mechanical metamaterial under a uniaxial strain of 50%, where the contour is displacement in the *y*-direction. (c) Genetic algorithm optimization history. The inset shows the structure of the optimal meta-atom. (d) and (e) are bandgap structures for the optimal metamaterial at free state and under uniaxial strain of 50%, respectively.

phononic bandgaps upon strains [54–57]. Four candidate shapes for the voids, including an equilateral triangle, a circle, a square, and a hexagon, were chosen, as shown in Fig. 3a. The length of the square matrix is 20 mm, and each meta-atom is composed of four bases. These voids are designed to have identical area and thus, their dimension  $s_1$ ,  $s_2$ ,  $s_3$ , and  $s_4$  are 16.16 mm, 12.00 mm, 10.63 mm, and 6.60 mm, respectively. The periodicity  $a_2$  is 80 mm. The Young's modulus, Poisson's ratio and mass density of the matrix is 3 MPa, 0.46 and 1130 kg/m³, respectively. The population size of 30 was used. A tensile force was applied on the soft 1D metamaterial along y-direction as shown in Fig. 3b.

The objective is to find out an arrangement of the four given voids so that a maximized tunable bandgap region could be achieved by applying a uniaxial tension strain of 50%. The fitness function  $f_2$  is the change of the maximized bandgap after a 50% strain is applied on the meta-atom and was given by  $\left|\Delta\omega^{free}-\Delta\omega^{def}\right|$ , where  $\Delta\omega^{free}$  and  $\Delta\omega^{def}$  are defined as

$$\begin{cases} \Delta \omega^{free} = \max[\min(\omega_{j+1}^{free}) - \max(\omega_{j}^{free})] \\ \Delta \omega^{def} = \max[\min(\omega_{j+1}^{def}) - \max(\omega_{j}^{def})] \end{cases} \qquad j = 1, 2 \dots 5$$
 (2)

where  $\omega_j^{free}$  and  $\omega_j^{def}$  are the frequency of jth band for the metaatom at the free and the 50% deformed state, respectively. The bandgap structure of the randomly generated initial configuration (Fig. 3a) and that under a 50% uniaxial tensile strain are plotted in Fig. S3, which shows the change of the maximized bandgap (i.e., from  $\Delta\omega_j^{free}$  to  $\Delta\omega_j^{def}$ ) upon deformation.

In this case, we just adopted GA optimization approach since the total possible configurations is rather small (i.e.,  $4^4 = 256$ ). The iteration history was given by Fig. 3c, from which one can observe that a meta-atom with a maximized range of tunable bandgap has been achieved at the 8th generation. The bandgap structure of the optimal meta-atom in free and the deformed state upon 50% uniaxial tensile strain are shown in Fig. 3d, and e, respectively. By comparing Fig. 3d and e, we can also see when the optimal meta-atom is deformed by applying a uniaxial strain of 50%, a will decrease and the range of b will increase. Therefore, the wave number range in Fig. 3e (deformed configuration of the optimal meta-atom) is larger than that of Fig. 3d (initial configuration of the optimal meta-atom). It is found that the phononic wave at frequency range of [255.50 Hz, 305.16 Hz] is forbidden

to propagate in the optimal one-dimensional metamaterial at the free state but can easily transmit through it upon a 50% tensile strain. This example clearly shows the discovery of a meta-atom with tunable bandgap structure upon deformation.

# 3.3. Case III: Maximizing relative bandgap for 2D phononic metamaterials

This example is a 2D case, a meta-atom consisting of a square matrix embedded with 9 layers of circular inclusions (Fig. 4a), and the 2D phononic metamaterial is the replication of the metaatoms in the planar direction. The radius of the largest circular inclusion R is 18 mm, and the increment of the radius  $\Delta r$  is 2 mm. The periodicity of the simulated model a equates 40 mm. The material of the matrix was given, while that of each layer was to be determined. Four candidate materials for the inclusion were provided, and their properties are listed in Fig. S2b. Thus, the total possible configurations is  $4^9 = 262$ , 144. Similar to the 1D case (Section 3.1), the relative width of bandgap is selected as the fitness function of the optimization process (e.g., Eq. (1)). Here, we also consider the first six bands. Both GA optimization and neural networks model were adopted for comparison.

The calculation process by the GA is shown in Fig. 4b. At the 30th generation, a maximized fitness function value of 1.098 was obtained and the corresponding structure of the optimal meta-atom is shown in the inset of Fig. 4b. The total accessed configurations in this process are  $30 \times 30 = 900$ , only a small fraction ( $\approx 0.3\%$ ) of the total configurations, showing the efficiency of the present method. Based on this meta-atom, a two-dimensional phononic metamaterial with maximized relative bandgap could be constructed. Fig. 4c shows the band structure of 2D metamaterial constructed by the optimal meta-atom. It has a bandgap between [119.03 Hz, 409.19 Hz], preventing wave propagation along all directions. We also studied the sensitivity of the initial configurations on the final result. We used different initial configurations and evolve to the same final state (Fig. S4).

Similar to case I, the neural networks model was also adopted to produce an optimal meta-atom. 1000 sample configurations were randomly created and used as training and testing data to train the neutral network model. Then, 100 meta-atom candidates were predicted, which are most likely to have large relative

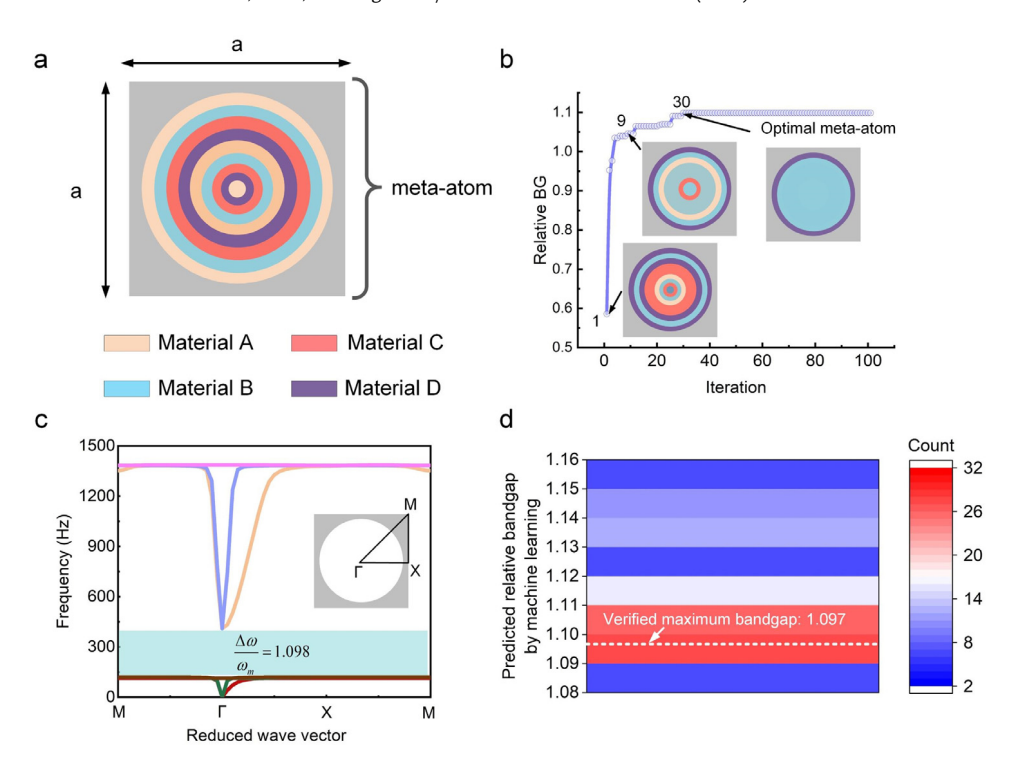


**Fig. 4.** A 2D phononic meta-atom with maximized relative bandgap. (a) A meta-atom consisting of nine layers of circular inclusions inside a square phononic matrix. (b) Genetic algorithm optimization history. The insets present the structure of best individual for the 1st, 9th, and 30th iteration generation, respectively. An optimal meta-atom is obtained in 30th generation. (c) Bandgap structure of the optimal meta-atom. (d) The predicted result produced by machine learning. The contour shows the number of configurations predicted by the machine learning method. The dashed line indicates the maximum bandgap as verified by the finite element simulation.

bandgap. Details can be found in supporting information. The result predicted by neural networks is shown in Fig. 4d, from which we can clearly see that the maximum predicted relative bandgap value is 1.097, which agrees well with the GA optimization.

# 3.4. Case IV: optimization design of interconnect for stretchable electronics

One of the most important topics in stretchable electronics is the development of stretchable interconnects to link the rigid functional devices [58-62]. In addition to large stretchability, other requirements for the interconnects may include smaller out-of-plane deformation and small electrical resistance. In this example, we selected 9 interconnect structural bases with different patterns and thicknesses as shown in Fig. S5a (also in Fig. 5a-c), namely spiral patterns (A), self-similar serpentine patterns (B), and serpentine patterns (C). Detailed geometry sizes can be found in literature [58]. For each pattern, three cross-sectional thicknesses (i.e., 1  $\mu$ m, 2  $\mu$ m, and 3  $\mu$ m) were assigned. For the sake of discussion, the subscripts 1 to 3 are used to denote the cross-sectional area. For example,  $A_1$  is the spiral pattern with 1 µm cross-sectional thickness. Our purpose is to obtain an optimal meta-atom composed by three units that are selected from the above-mentioned 9 structural bases, as shown in Fig. S5b. An example of meta-atom composed by  $A_1$ ,  $B_1$  and  $C_1$  is presented in Fig. S5c. We defined a figure of merit to evaluate the performance of the meta-atom, i.e., the fitness function  $f_4$  by

$$f_4 = \frac{(S|_{\text{max.}prin=1\%})^4}{\omega \cdot R}$$
 (3)

where  $\omega$  is the maximum out-of-plane displacement during the stretching process in mm,  $S|_{\max.prin=1\%}$  is the maximum applied strain when the maximum principal strain in the interconnects reaches 1%, R is the electrical resistance of interconnects in  $\Omega$ .

To simplify the analysis, we assume that R takes the value of 1, 1/2, and 1/3 when the cross-sectional thicknesses thickness of interconnects equals to 1  $\mu$ m, 2  $\mu$ m, and 3  $\mu$ m, respectively. It must be pointed out that this figure of merit was solely to implement the present modular design method and its physical meaning only superficially reflects the possible need to optimize the stretchable interconnects. The rationale of the figure of merit is not the concern of this paper.

The material parameters are Young's modulus of 119 GPa and Poisson's ratio of 0.34. Here, we did not consider the plasticity of the material. The finite element results for  $A_1$ ,  $B_1$  and  $C_1$  are shown in Fig. 5a–c, respectively. The results for other 6 structural bases  $(A_2, B_2, C_2, A_3, B_3, C_3)$  are presented in Figs. S6–S11, respectively.

Here, the neural networks model was used to find the optimal configuration. 95 samples with random configurations of meta-atoms was constructed and their fitness functions were calculated. Then those data were utilized as the input data to train the neural networks model. Details could be found in the supporting information. The result predicted by machine learning is shown in Fig. 5d, from which one can clearly see that the maximum predicted value of  $f_4$  is 124.01, which corresponds to an optimal meta-atom with configuration of  $A_2A_2A_2$ . The relationship between its maximum out-of-plane displacement and applied strain is shown in Fig. 5e, while the relationship between the maximum principal strain and applied strain is shown in Fig. 5f. This optimal meta-atom offers large stretch ability, small out-of-plane displacement and small electrical resistance.

### 4. Concluding remarks

This Letter introduces the machine-learning based method for the design of modular metamaterials with specified properties. The method combines performance evaluation together

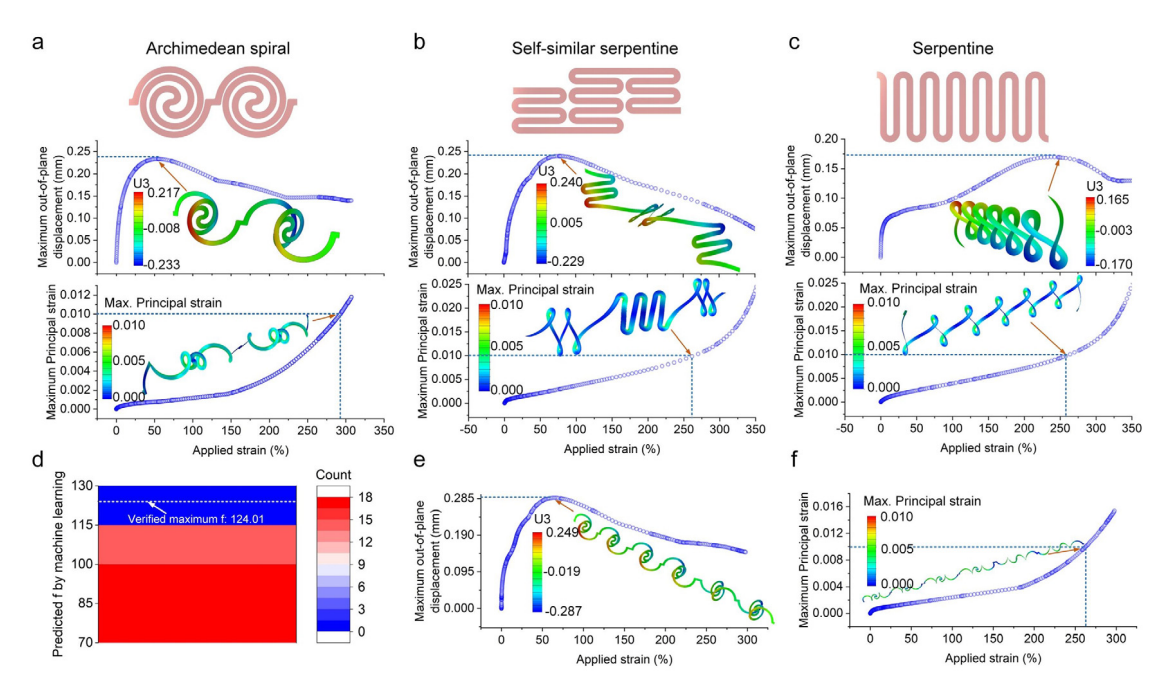


**Fig. 5.** Meta-atom design of interconnect for stretchable electronics. The structure pattern, the relationship between maximum out-of-plane displacement and applied strain, and the relationship between maximum principal strain with applied strain for (a) Archimedean spiral pattern, (b) self-similar serpentine pattern, and (c) serpentine pattern. (d) The predicted result produced by machine learning. The contour shows the number of configurations predicted by the machine learning method. The dashed line indicates the maximum bandgap as verified by the finite element simulation. (e) The relationship between maximum out-of-plane displacement and applied strain. (f) The relationship between maximum principal strain and applied strain for the predicted optimal meta-atom. The insets for (a-c) and (e-f) are the corresponding deformation configuration calculated by FEA simulation.

with structural evolution to construct meta-atoms with optimal performance based on the preselected structural bases. Four case studies have been provided to demonstrate the implementation of the present method. The results show that the present method can take advantage of the existing knowledge of metamaterials from the ad hoc method or the topology optimization method and offer an effective means to design modular metamaterials. Though the demonstration is just for mechanical metamaterials, it is believed that the machine learning-based method and the concept of modular metamaterials are capable to construct meta-atoms with specific properties for metamaterials in various fields.

Like any design methods, the present method also has some limitations. Though the preselection of the structural basis endows the modular method the ability to effectively achieve the desired meta-atom, the selection itself has also limited the possibility to include other configurations that are either not chosen from the existing knowledge base or not discovered yet. Thus, to apply this method to design meta-atoms, one needs to extensively comprehend the existing knowledge in order to preselect proper structural basis. In other words, the present modular design provides an engineering methodology to harness the comprehended knowledge on metamaterials to effectively design new meta-atoms with desired performance.

### **Declaration of competing interest**

The authors declare that they have no known competing financial interests or personal relationships that could have appeared to influence the work reported in this paper.

#### Acknowledgements

LW acknowledges the Foundation for Distinguished Young Talents in Higher Education of Guangdong Province, China under Grant No. 2018KQNCX269 and the Special Funds for the Cultivation of Guangdong College Students' Scientific and Technological Innovation, China under Grant No. pdjh2020b0598. YW acknowledges the National Natural Science Foundation of China under Grant Nos. 11872328, 11532011 and 11621062, and the Fundamental Research Funds for the Central Universities, China under Grant No. 2018FZA4025. QW acknowledges the National Key R&D Program of China under Grant No. 2018YFB1201601. HJ acknowledges the support from the National Science Foundation, USA (CMMI-1762792).

### Appendix A. Supplementary data

Supplementary material related to this article can be found online at https://doi.org/10.1016/j.eml.2020.100657.

#### References

- [1] D.R. Smith, J.B. Pendry, M.C.K. Wiltshire, Metamaterials and negative refractive index, Science 305 (5685) (2004) 788–792.
- [2] N. Fang, D. Xi, J. Xu, M. Ambati, W. Srituravanich, C. Sun, X. Zhang, Ultrasonic metamaterials with negative modulus, Nature Mater. 5 (6) (2006) 452–456.
- [3] V.M. Shalaev, Optical negative-index metamaterials, Nat. Photonics 1 (1) (2007) 41–48.
- [4] W. Cai, U.K. Chettiar, A.V. Kildishev, V.M. Shalaev, Optical cloaking with metamaterials, Nat. Photonics 1 (4) (2007) 224–227.
- [5] M. Wegener, Metamaterials beyond optics, Science 342 (2013) 3.
- [6] T. Kanit, S. Forest, I. Galliet, V. Mounoury, D. Jeulin, Determination of the size of the representative volume element for random composites: statistical and numerical approach, Int. J. Solids Struct. 40 (13) (2003) 3647–3679.
- [7] C.M. Soukoulis, S. Linden, M. Wegener, Negative refractive index at optical wavelengths, Science 315 (5808) (2007) 47–49.
- [8] P.Y. Chen, M. Farhat, A. Alu, Bistable and self-tunable negative-index metamaterial at optical frequencies, Phys. Rev. Lett. 106 (10) (2011) 105503
- [9] D. Schurig, J.J. Mock, B.J. Justice, S.A. Cummer, J.B. Pendry, A.F. Starr, D.R. Smith, Metamaterial electromagnetic cloak at microwave frequencies, Science 314 (5801) (2006) 977–980.

- [10] D. Shin, Y. Urzhumov, Y. Jung, G. Kang, S. Baek, M. Choi, H. Park, K. Kim, D.R. Smith, Broadband electromagnetic cloaking with smart metamaterials, Nature Commun. 3 (2012).
- [11] J.B. Pendry, Negative refraction makes a perfect lens, Phys. Rev. Lett. 85 (18) (2000) 3966–3969.
- [12] K. Bertoldi, P.M. Reis, S. Willshaw, T. Mullin, Negative Poisson's ratio behavior induced by an elastic instability, Adv. Mater. 22 (3) (2010) 361.
- [13] S. Babaee, J. Shim, J.C. Weaver, E.R. Chen, N. Patel, K. Bertoldi, 3D soft metamaterials with negative Poisson's ratio, Adv. Mater. 25 (36) (2013) 5044–5049.
- [14] J.N. Grima, S. Winczewski, L. Mizzi, M.C. Grech, R. Cauchi, R. Gatt, D. Attard, K.W. Wojciechowski, J. Rybicki, Tailoring graphene to achieve negative Poisson's ratio properties, Adv. Mater. 27 (8) (2015) 1455–1459.
- [15] T.A. Hewage, K.L. Alderson, A. Alderson, F. Scarpa, Double-negative mechanical metamaterials displaying simultaneous negative stiffness and negative Poisson's ratio properties, Adv. Mater. 28 (46) (2016) 10323–10332.
- [16] R. Lakes, Cellular solid structures with unbounded thermal expansion, 15 (1996) 3.
- [17] W. Miller, C.W. Smith, D.S. Mackenzie, K.E. Evans, Negative thermal expansion: a review, J. Mater. Sci. 44 (20) (2009) 5441–5451.
- [18] J.N. Grima, B. Ellul, R. Gatt, D. Attard, Negative thermal expansion from disc, cylindrical, and needle shaped inclusions, Phys. Status Solidi (b) (2013) n/a.
- [19] Q. Wang, J.A. Jackson, Q. Ge, J.B. Hopkins, C.M. Spadaccini, N.X. Fang, Lightweight mechanical metamaterials with tunable negative thermal expansion, Phys. Rev. Lett. 117 (17) (2016).
- [20] S.A. Cummer, J. Christensen, A. Alù, Controlling sound with acoustic metamaterials, Nat. Rev. Mater. 1 (3) (2016).
- [21] X. Yu, J. Zhou, H. Liang, Z. Jiang, L. Wu, Mechanical metamaterials associated with stiffness, rigidity and compressibility: A brief review, Prog. Mater. Sci. 94 (2018) 114–173.
- [22] P. Wang, F. Casadei, S. Shan, J.C. Weaver, K. Bertoldi, Harnessing buckling to design tunable locally resonant acoustic metamaterials, Phys. Rev. Lett. 113 (1) (2014) 014301.
- [23] A. Srivastava, Elastic metamaterials and dynamic homogenization: a review, Int. J. Smart Nano Mater. 6 (1) (2015) 41–60.
- [24] S. Krödel, N. Thomé, C. Daraio, Wide band-gap seismic metastructures, Extreme Mech. Lett. 4 (2015) 111–117.
- [25] S.A. Cummer, J. Christensen, A. Alù, Controlling sound with acoustic metamaterials, Nat. Rev. Mater. 1 (2016) 16001.
- [26] G. Ma, P. Sheng, Acoustic metamaterials: From local resonances to broad horizons, Sci. Adv. 2 (2) (2016) e1501595.
- [27] J. Cha, K.W. Kim, C. Daraio, Experimental realization of on-chip topological nanoelectromechanical metamaterials, Nature 564 (7735) (2018) 229–233.
- [28] V.M. García-Chocano, L. Sanchis, A. Díaz-Rubio, J. Martínez-Pastor, F. Cervera, R. Llopis-Pontiveros, J. Sánchez-Dehesa, Acoustic cloak for airborne sound by inverse design, Appl. Phys. Lett. 99 (7) (2011) 074102.
- [29] L. Zigoneanu, B.-I. Popa, S.A. Cummer, Three-dimensional broadband omnidirectional acoustic ground cloak, Nature Mater. 13 (2014) 352.
- [30] J. Li, C.T. Chan, Double-negative acoustic metamaterial, Phys. Rev. E 70 (5) (2004) 055602.
- [31] Y. Xie, B.-I. Popa, L. Zigoneanu, S.A. Cummer, Measurement of a broadband negative index with space-coiling acoustic metamaterials, Phys. Rev. Lett.
- 110 (17) (2013) 175501.
  [32] J.F. Robillard, J. Bucay, P.A. Deymier, A. Shelke, K. Muralidharan, B. Merheb, J.O. Vasseur, A. Sukhovich, J.H. Page, Resolution limit of a phononic crystal superlens, Phys. Rev. B 83 (22) (2011) 224301.
- [33] M. Molerón, C. Daraio, Acoustic metamaterial for subwavelength edge detection, Nature Commun. 6 (2015) 8037.
- [34] Y. Wang, B. Yousefzadeh, H. Chen, H. Nassar, G. Huang, C. Daraio, Observation of nonreciprocal wave propagation in a dynamic phononic lattice, Phys. Rev. Lett. 121 (19) (2018) 194301.
- [35] J.H. Oh, Y.K. Ahn, Y.Y. Kim, Maximization of operating frequency ranges of hyperbolic elastic metamaterials by topology optimization, Struct. Multidiscip. Optim. 52 (6) (2015) 1023–1040.
- [36] A. Clausen, F. Wang, J.S. Jensen, O. Sigmund, J.A. Lewis, Topology optimized architectures with programmable Poisson's ratio over large deformations, Adv. Mater. 27 (37) (2015) 5523–5527.
- [37] H. Zhang, Y. Luo, Z. Kang, Bi-material microstructural design of chiral auxetic metamaterials using topology optimization, Compos. Struct. 195 (2018) 232–248
- [38] H.-W. Dong, S.-D. Zhao, P. Wei, L. Cheng, Y.-S. Wang, C. Zhang, Systematic design and realization of double-negative acoustic metamaterials by topology optimization, Acta Mater. 172 (2019) 102–120.

- [39] W. Lin, J.C. Newman, W.K. Anderson, X. Zhang, Broadband shape and topology optimization of acoustic metamaterials and phononic crystals, in: 17th AIAA/ISSMO Multidisciplinary Analysis and Optimization Conference.
- [40] H.H. Huang, C.T. Sun, Wave attenuation mechanism in an acoustic metamaterial with negative effective mass density, New J. Phys. 11 (1) (2009) 013003
- [41] Z. Yang, H.M. Dai, N.H. Chan, G.C. Ma, P. Sheng, Acoustic metamaterial panels for sound attenuation in the 50–1000 Hz regime, Appl. Phys. Lett. 96 (4) (2010) 041906.
- [42] C.J. Naify, C.-M. Chang, G. McKnight, S. Nutt, Transmission loss and dynamic response of membrane-type locally resonant acoustic metamaterials, J. Appl. Phys. 108 (11) (2010) 114905.
- [43] M. Yang, G. Ma, Z. Yang, P. Sheng, Coupled membranes with doubly negative mass density and bulk modulus, Phys. Rev. Lett. 110 (13) (2013) 134301.
- [44] S. Zhang, L. Yin, N. Fang, Focusing ultrasound with an acoustic metamaterial network, Phys. Rev. Lett. 102 (19) (2009) 194301.
- [45] A. White, The materials genome initiative: One year on, MRS Bull. 37 (8) (2012) 715–716.
- [46] R. Arróyave, D.L. McDowell, Systems approaches to materials design: Past, present, and future, Annu. Rev. Mater. Res. 49 (1) (2019) 103–126.
- [47] M. Yim, W. Shen, B. Salemi, D. Rus, M. Moll, H. Lipson, E. Klavins, G.S. Chirikjian, Modular self-reconfigurable robot systems [Grand challenges of robotics], IEEE Robot. Autom. Mag. 14 (1) (2007) 43–52.
- [48] W. Yang, Q. Liu, Z. Gao, Z. Yue, B. Xu, Theoretical search for heterogeneously architected 2D structures, Proc. Natl. Acad. Sci. USA 115 (31) (2018) E7245–E7254.
- [49] K. Bertoldi, M.C. Boyce, Mechanically triggered transformations of phononic band gaps in periodic elastomeric structures, Phys. Rev. B 77 (5) (2008) 052105
- [50] J.R. Koza, Genetic Programming: On the Programming of Computers by Means of Natural Selection, MIT Press, 1992, p. 680.
- [51] J.O. Vasseur, P.A. Deymier, G. Frantziskonis, G. Hong, B. Djafari-Rouhani, L. Dobrzynski, Experimental evidence for the existence of absolute acoustic band gaps in two-dimensional periodic composite media, J. Phys.: Condens. Matter 10 (27) (1998) 6051–6064.
- [52] J.O. Vasseur, P.A. Deymier, B. Chenni, B. Djafari-Rouhani, L. Dobrzynski, D. Prevost, Experimental and theoretical evidence for the existence of absolute acoustic band gaps in two-dimensional solid phononic crystals, Phys. Rev. Lett. 86 (14) (2001) 3012–3015.
- [53] Y. Pennec, J.O. Vasseur, B. Djafari-Rouhani, L. Dobrzyński, P.A. Deymier, Two-dimensional phononic crystals: Examples and applications, Surf. Sci. Rep. 65 (8) (2010) 229–291.
- [54] P. Wang, J. Shim, K. Bertoldi, Effects of geometric and material nonlinearities on tunable band gaps and low-frequency directionality of phononic crystals, Phys. Rev. B 88 (1) (2013) 014304.
- [55] S. Shan, S.H. Kang, P. Wang, C. Qu, S. Shian, E.R. Chen, K. Bertoldi, Harnessing multiple folding mechanisms in soft periodic structures for tunable control of elastic waves, Adv. Funct. Mater. 24 (31) (2014) 4935–4942.
- [56] P. Zhang, W.J. Parnell, Soft phononic crystals with deformationindependent band gaps, Proc. Math. Phys. Eng. Sci. 473 (2200) (2017) 20160865.
- [57] N. Gao, J. Li, R.H. Bao, W.Q. Chen, Harnessing uniaxial tension to tune Poisson's ratio and wave propagation in soft porous phononic crystals: an experimental study, Soft Matter. 15 (14) (2019) 2921–2927.
- [58] C. Lv, H. Yu, H. Jiang, Archimedean spiral design for extremely stretchable interconnects, Extreme Mech. Lett. 1 (2014) 29–34.
- [59] Y. Zhang, H. Fu, S. Xu, J.A. Fan, K.-C. Hwang, J. Jiang, J.A. Rogers, Y. Huang, A hierarchical computational model for stretchable interconnects with fractal-inspired designs, J. Mech. Phys. Solids 72 (2014) 115–130.
- [60] Y. Zhang, H. Fu, Y. Su, S. Xu, H. Cheng, J.A. Fan, K.-C. Hwang, J.A. Rogers, Y. Huang, Mechanics of ultra-stretchable self-similar serpentine interconnects, Acta Mater. 61 (20) (2013) 7816–7827.
- [61] D.-H. Kim, J. Song, W.M. Choi, H.-S. Kim, R.-H. Kim, Z. Liu, Y.Y. Huang, K.-C. Hwang, Y.-w. Zhang, J.A. Rogers, Materials and noncoplanar mesh designs for integrated circuits with linear elastic responses to extreme mechanical deformations, Proc. Natl. Acad. Sci. 105 (48) (2008) 18675–18680.
- [62] S. Xu, Y. Zhang, J. Cho, J. Lee, X. Huang, L. Jia, J.A. Fan, Y. Su, J. Su, H. Zhang, H. Cheng, B. Lu, C. Yu, C. Chuang, T.-i. Kim, T. Song, K. Shigeta, S. Kang, C. Dagdeviren, I. Petrov, P.V. Braun, Y. Huang, U. Paik, J.A. Rogers, Stretchable batteries with self-similar serpentine interconnects and integrated wireless recharging systems, Nature Commun. 4 (1) (2013) 1543.